EasyChair Preprint

№ 13405

Frame Structures Damage Detection System and Evaluation Method Based on Twist Slit Damper Plastic Energy Dissipation

Haoda Teng, Riku Fujie, Natsuhiko Sakiyama,
Haruna Hiromatsu, Yuki Jin, Takumi Ito and Donghang Wu

May 21, 2024

Frame Structures Damage Detection System and Evaluation Method Based on Twist Slit Damper Plastic Energy Dissipation

Haoda Teng[1], Riku Fujie[1], Natsuhiko Sakiyama[1], Haruna Hiromatsu[1], Yuki Jin[1], Takumi Ito[1] and Donghang Wu[2]

[1] Department of Architecture, Tokyo University of Science, Tokyo, Japan.
2 WU Building Office Corporation, Tokyo, Japan.

thd01@hotmail.com

Abstract.
After a severe earthquake disaster, the building structure will be seriously damaged by the seismic force. Applying plastic energy dissipation of members with IoT functionality is an excellent technique to swiftly assess the structure's remaining life.

In the previous study, a method to evaluate the cumulative damage degree of steel was proposed through the reverse analysis of the heat generation characteristics of steel plastic deformation.

This paper proposes a damage detection system, based on the damper's plastic energy dissipation. Due to the rigidity of the column, setting dampers directly on the column cannot effectively exert its function. By setting columns both ends of which are hinged in the frame and installing knee dampers on them, it is possible to evaluate the drift angle and damage degree of the frame structure better. We place this damage detection system in the loading frame to apply static cyclic loads. With the drift angle as the target, the inverse analysis of the temperature rise which is measured by sensors caused by a damper in plastic deformation can be carried out, and the drift angle of the frame structure can be calculated.

This damage detection system can display in real time the drift angle, the column foot's cumulative plastic damage, and the instant when the plastic hinge first appears.

Keywords: Steel framed structure, Seismic disaster, Structural health monitoring, Internet of Things, Plastic thermal behavior.

1 Introduction

After the earthquake, to confirm the damage degree of buildings in the disaster area and the safety of refuge facilities, it is necessary to let experts conduct an emergency risk assessment [1] and disaster severity classification adjustment [2]. However, infrastructural damages might prevent the investigators from reaching the earthquake disaster area. In recent years, with the development of IOT sensors, the distant monitoring and communication technology of structural health monitoring is also developing.

Because of the influence of non-structural components, the damage of structural components is difficult to measure by sensors such as accelerometers.

In previous studies, a damage evaluation method based on heat generation characteristics of steel plastic deformation (hereinafter referred to as plastic thermal behavior) and temperature changes caused by elastic deformation (thermoelastic effect) [3, 4] was proposed and verified. Because of the fire-resistant coating of the steel structures, it is difficult to directly use the plastic thermal behavior to evaluate the damage to the steel components.

This paper proposed the damage detection system of the hinged column and the frame with knee damper by the plastic thermal behavior of the energy dissipation member.

2 Frame damage detection system and Twist Slit Damper

Based on previous research [5], the failure model of damping frame structure is proposed, as shown in Figure 1. However, because the beam-column joints of buildings are designed to have relatively high rigidity in actual construction projects, the angle of beam-column joints will not deform greatly when subjected to an earthquake. This paper proposes a damage detection system for the frame structures with hinged columns and knee dampers as shown in Figure 2.

The thermoelectric device (Fig. 3) is installed on the surface of the energy dissipation member to measure the temperature change of the knee damper under plastic deformation. The thermoelectric devices will output the temperature difference between the two contact surfaces in the form of voltage. Minicomputers such as Raspberry PI (Fig. 4) will be used to receive and analyze the voltage data to calculate structural damage. Finally, through the Wi-Fi, 5g Network, or Bluetooth communication function of the minicomputer, the calculated structural damage data is sent to the digital terminal of the building owner or researcher to achieve the function of real-time monitoring and notification.

Toyosada [6] proposed that about 90% of the energy absorbed by plastic deformation is converted into heat energy, while Nakashima [7] confirmed the relationship between cumulative plastic deformation of steel and temperature change. Based on the plastic thermal behavior of the steel (Formula (1), (2); Fig.5), the plastic deformation of steel can be known.

$$\Delta T = 90\% E_P \tag{1}$$

$$E_P = \int_{\delta_1}^{\delta_2} P_1(\delta) \tag{2}$$

ΔT: Temperature change by measured;
E_P: Energy absorbed by plastic deformation;

The formula for evaluating the frame's drift angle with the damper's deformation is proposed, as shown in Formula (3).

$$R = \frac{\Delta l}{l \sin\theta \cos\theta} \tag{3}$$

R: Drift angle; l: Length of knee damper;
Δl: Deformation of knee damper; θ: Angle between knee damper and hinged column.

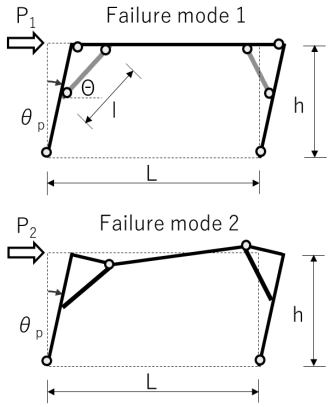

Fig. 1. Failure modes of a frame model with a knee damper

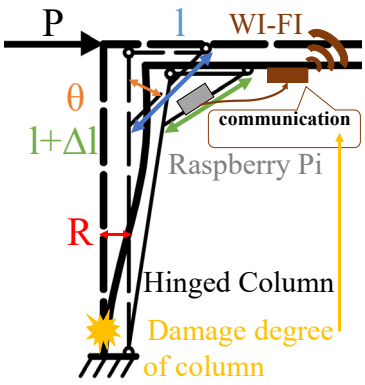

Fig. 2. Damage detection system with hinged column and knee damper

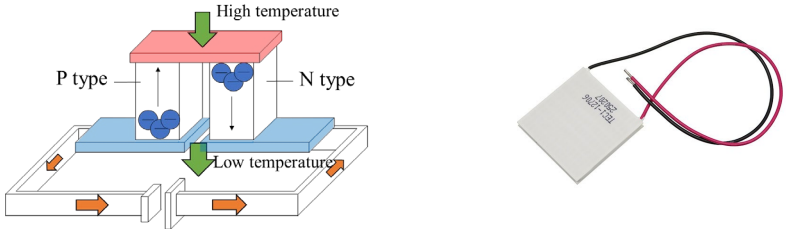

Fig. 3. Thermoelectric device

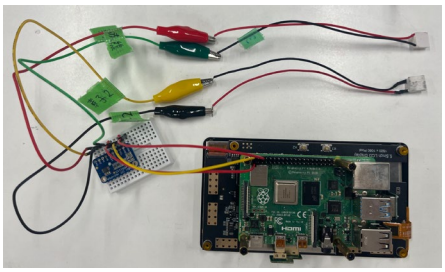

Fig. 4. Photo of Raspberry pi and thermoelectric device

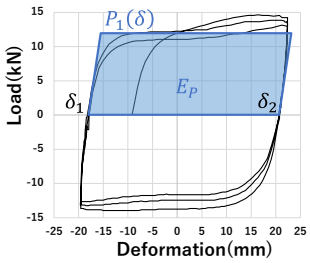

Fig. 5. Energy absorbed by plastic deformation

The steel knee damper is used as the energy dissipation component, and the plastic deformation of the damper is calculated by measuring its plastic thermal behavior.

However considering the strength of the knee damper, it affects the design of the hinged column and its joint. Also, as the steel will produce plastic hardening after yielding, it is very disadvantageous for us to analyze the thermal behavior. This paper proposes a kind of slit damper after torsion, called the ***Twist Slit Damper*** (Hereinafter referred to as *the TSD*). Formula (4) can be used to analyze the mechanical properties of the TSD by section modulus.

$$Z = \frac{bh(b^2\cos^2\theta + h^2\sin^2\theta)}{6(b\cos\theta + h\sin\theta)} \quad (4\text{-a})$$

$$M_y = \sigma_y Z \quad (4\text{-b})$$

$$M_x = M_{px}\left(1 - \frac{b^2\tan^2\theta}{3h^2}\right) \quad (4\text{-c})$$

$$M_y = \frac{2b\,M_{py}\tan\theta}{3h} \quad (4\text{-d})$$

$$M_{px} = Z_{px}\sigma_y \quad (4\text{-e})$$

$$M_{py} = Z_{py}\sigma_y \quad (4\text{-f})$$

b,h: shown in Figure 12(a);θ: Torsional angle; Z : Section modulus;
Z_p: Plastic section modulus; σ_y: Yield stress; M_y: Yield moment;
M_x, M_y : moment of X, Y-axis under biaxial bending;
M_{px}, M_{py}: fully plastic moment of X, Y-axis under biaxial bending.

Due to the large initial plastic deformation, the limit strength is not too high, so the appropriate size of the TSD can be installed on the steel square rod with slide rail (Fig. 6). The slide rail can ensure that the deformation of the square rod has a high correlation with the deformation of the frame structure. The energy absorbed by the plastic deformation of the TSD set on the square rod is also related to the deformation of the frame structure. Therefore, the damage degree of the frame structure can be evaluated by the plastic thermal behavior by the TSD. (Fig. 7)

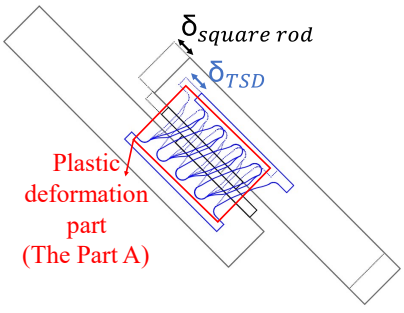

Fig. 6. Square rod with slide rail and TSD

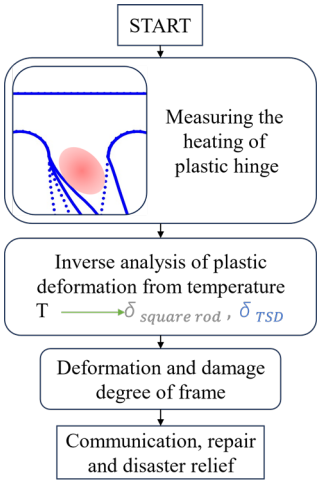

Fig. 7. Program of damage evaluation method

3 Experiment summary

3.1 Frame experiment

Experiment summary

As shown in Figure 8, a frame experiment using hinged columns and square rods as a damage detection system was set up, and an H-shaped steel test body was used as the evaluated component.

The upper and lower ends of H-shaped steel are rigidly combined with ten high-strength bolts to simulate the rigid bonding nodes of actual buildings. The square rod with slide rail is set on the hinged column and beam of the evaluation system.

By measuring the deformation of the square rod, the drift angle of the column can be inferred, and then the damage of the column can be inferred.

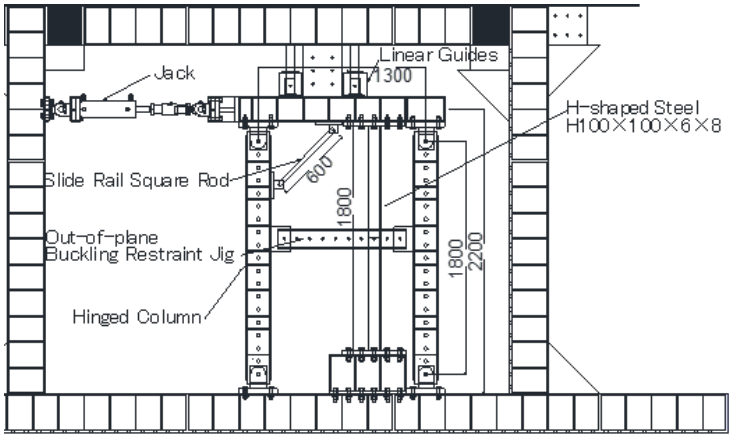

Fig. 8. Setup of frame experiment

Summary of experimental body

The mechanical properties and figure of H-shaped steel are shown in Figure 9 and Table 1, which is welded by steel plate (Steel SN400B).

The square rod is shown in Figure 10. By using stripper bolts, bearings, and sliding rails, the deformation of the square rod can be measured accurately.

Table 1. Mechanical properties of H-shaped steel.

	Young's modulus (N/mm^2)	yield strength (N/mm^2)	strength of extension (N/mm^2)	yield strain (μ)
flange	196405	357	495	1813
web	181584	315	468	1879

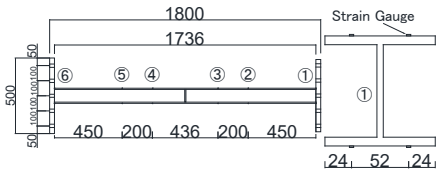

Fig. 9. Figure of H-shaped steel

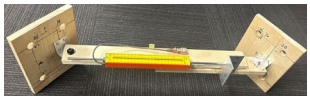

Fig. 10(a). Photo of square rod

Fig. 10(b). Photo of the slide rail

Loading plan and measurement plan

As shown in Figure 8, the horizontal loading test is carried out with the drift angle as the target. The loading plan is incremental loading, and the drift angle is 1/500, 1/200, 1/150, 1/100, 1/75, 1/50 and 1/30 rad. The loading is carried out twice each time, and the last round is loaded to the limit of the Jack.

3.2 Element experiment of the TSD

Experiment summary

Because the mechanical properties of the TSD needs to be understood, TSDs were enlarged by 3-4 times and carried out the element experiment according to the setting shown in Figure 11.

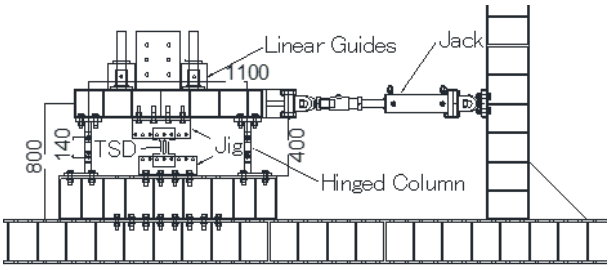

Fig. 11. Setup of element experiment

Summary of experimental body

The figure and mechanical properties of the TSDs (Steel SS400) are shown in Figure 12 and Table 2. *The Part A** is clamped by a sheet metal tool and twisted in one direction. TSDs are divided into five test bodies from 0 ° to 90 ° according to the torsional angle of the Part A.

(***The Part A*** is shown in Fig. 6)

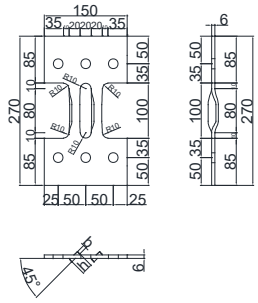

Fig. 12(a). The figure of the enlarged TSD

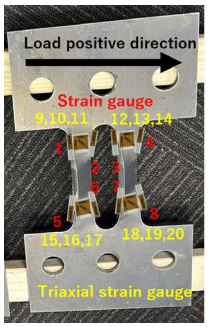

Fig. 12(b). Photo of the enlarged TSD

Table 2. Mechanical properties of the TSD.

Young's modulus (N/mm^2)	yield strength (N/mm^2)	strength of extension (N/mm^2)	yield strain (μ)
210627	388	450	1887

Table 3. Names of the TSD.

	monotonic loading					cyclic loading		
Torsional angle of the Part A	0°	30°	45°	60°	90°	30°	45°	60°
Name of the TSD	N-0	N-30	N-45	N-60	N-90	R-30	R-45	R-60

Loading plan and measurement plan

Considering the torsion direction of The Part a, different loading directions may have different mechanical properties. Therefore, it is necessary to define the positive loading direction of TSDs. As shown in Figure 12 (b), the direction of the arrow is the positive loading direction.

Firstly, N-30, N-45 and N-60 were monotonically loaded in the positive direction, and von Mises stress was obtained by triaxial strain gauges at both ends of The Part A.

Because only the plane stress-strain state is considered, the evaluation formula of the two-dimensional plane is shown in Formula (5).

$$\sigma_{Mises}^2 = \frac{(\sigma_{max}-\sigma_{min})^2+(\sigma_{max})^2+(\sigma_{min})^2}{2} \tag{5-a}$$

$$\sigma_{max} = \frac{E}{2}\left[\frac{\varepsilon_1+\varepsilon_2}{1-\nu} + \frac{1}{1+\nu}\sqrt{2\{(\varepsilon_1-\varepsilon_3)^2+(\varepsilon_2-\varepsilon_3)^2\}}\right] \tag{5-b}$$

$$\sigma_{min} = \frac{E}{2}\left[\frac{\varepsilon_1+\varepsilon_2}{1-\nu} - \frac{1}{1+\nu}\sqrt{2\{(\varepsilon_1-\varepsilon_3)^2+(\varepsilon_2-\varepsilon_3)^2\}}\right] \tag{5-c}$$

σ_{Mises} : Von Mises Stress;σ_{max}: Maximum principal stress;
σ_{min} : Minimum principal stress; $\varepsilon_1, \varepsilon_2, \varepsilon_3$: Strain of triaxial strain gauge.

The deformation when Von Mises stress reaches the yield strength of the material is regarded as the plasticity rate 1, and the cyclic loading is carried out with the plasticity rate of 0.25,0.5,1,2,4,8,12,16,20,40 as the target. Each round is loaded three times. When the maximum load is reduced to 90% of the previous load plan, the next loop is the final loop.

Then N-0 and N-90 were loaded in the positive direction as the control group, and then loaded in the negative direction.

4 Experiment Results and Analysis

4.1 Frame experiment

Load-Deformation curve

Since the energy dissipation member is not installed on the square staff, the square staff does not bear the load. As shown in Figure 13, the Load-Displacement curve of the damage detection system shows the mechanical properties of H-shaped steel.

Drift angle curve

In Figure 14, the drift angle can be determined by measuring the horizontal displacement and the square rod deformation.

From Figure 6, the displacement of the TSD is the same as that of the square rod. As shown in Figure 2 and Formula (3), the drift angle of the structure can be calculated by the displacement of the square rod. And from Figure 5 and Formulas (1), (2), the plastic deformation of the TSD can be calculated by measuring TSDs' heat generation characteristics, so that the drift angle of the structure can be evaluated by using the heat generation characteristics of TSDs' plastic deformation.

However, due to the influence of the clearance of the bolt hole and the length of the gusset plate, the actual analysis results will not be very accurate. These errors can be easily removed in the laboratory, but it is very difficult to remove these errors in the actual building structure. This is the next topic to consider.

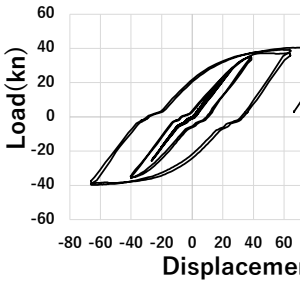

Fig. 13. Load-Deformation curve

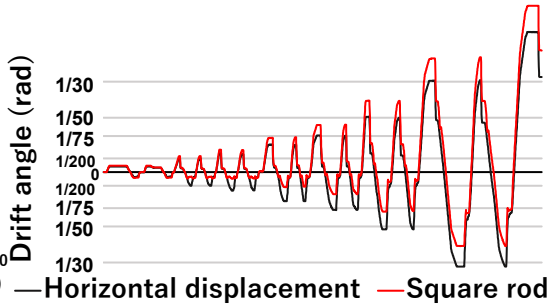

Fig. 14. Drift angle curve

4.2 Element experiment of the TSD

Load-Deformation curve

Because the TSD has a large initial plastic deformation before loading, and the softening effect of the yield platform has occurred, it is difficult to determine the yield strength directly. The general yield point method was selected to determine the plastic strength of the TSD. (Fig. 15)

From Figure 16, From the curve of the monotonic experiment, the plastic strength, initial rigidity, and displacement (Table 4) when each TSDs are yielded can be known. The yield strength and rigidity are related to the initial plastic deformation and decrease with the increase of the initial torsional angle.

From the monotonic experiment, it can be found that the torsional angle of The Part A will change with loading, so such a jig used to obtain the torsional angle of The Part A is set, as shown in Figure 17.

According to the results of the monotonic experiment, the cyclic experiment was carried out, as shown in Figure 18. In the second half of the loading, the load of TSDs have a negative slope and a serious load degradation phenomenon is found. As shown in Figure 19, the photo of R-60 after cyclic loading shows that the torsional angle of The Part A has exceeded 90 °.

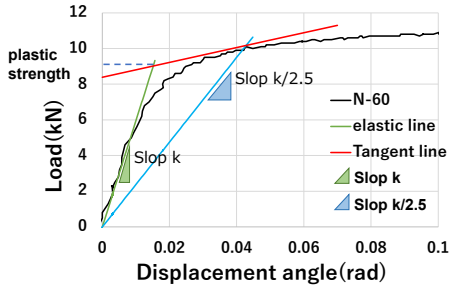

Fig. 15. General yield point method of N-60

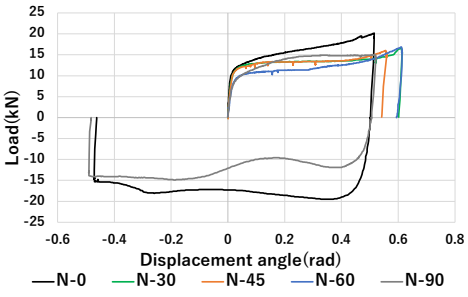

Fig. 16. Load-Deformation angle curve

Table 4. Characteristics of the TSD.

Name of the TSD	Initial rigidity (kN/rad)	Displacement of plasticity rate 1(mm)	Plastic strength (kN)
N-0	1153.9	2.70	10.8
N-30	916.7	2.00	10.6
N-45	789.5	2.80	10.7
N-60	593.8	1.20	9.0
N-90	497.1	1.10	8.4

Fig. 17. Photos of the jig

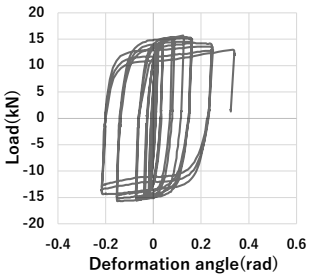

Fig. 18(a). R-30 Load-Deformation angle curve

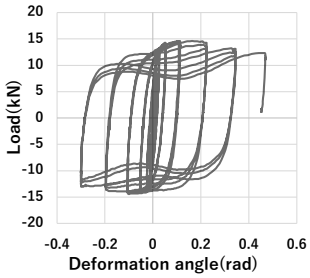

Fig. 18(b). R-45 Load-Deformation angle curve

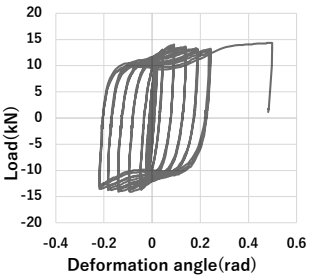

Fig. 18(c). R-60 Load-Deformation angle curve

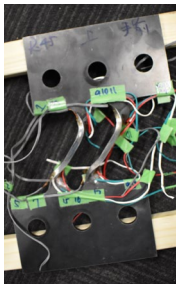

Fig. 19. Photo of the loaded R-60

Relationship between torsional angle and load

At present, the research on the torsion of large plastic deformation has not been clear, Therefore, the change of torsional rigidity during loading under large torsional deformation cannot be determined. However, due to the section modulus of The Part A in the loading process, the hardening relationship of the section from yield to fully yield can be calculated. By comparing the monotonic experiment with the cyclic experiment, the strain hardening relationship of large torsional plastic deformation under load can also be obtained.

As shown in Figure 20, the load is converted into the moment of the lower end of The Part A and obtained its envelope curve. On this basis, the theoretical plastic moment and theoretical fully plastic moment of The Part A at each torsional angle can be calculated through the section modulus Z, ZP (Formula (4)) [8]. The correlation between to load and torsional angle can be obtained.

Due to the large plastic deformation, it is difficult to calculate the moment from the strain. The strain at the lower end of The Part A on the strong axis side (No. 5 and No. 6 strain gauges in Fig. 12 (b)) is converted into curvature for comparison. In particular, the data at the unloading point of the cyclic experimental loop is made into an envelope.

From Figure 21, the curvature of The Part A when the load is stable during the loading and the hardening rate under the same curvature within this range (Table 5) can be obtained. When TSDs are loaded, the reduction of section modulus determined by torsional angle will reduce the strength of the TSDs, which will offset the plastic hardening effect of steel.

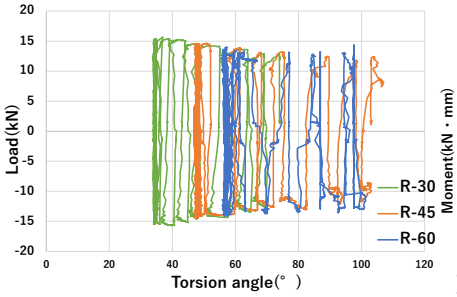

Fig. 20(a). Load-Torsional angle curve

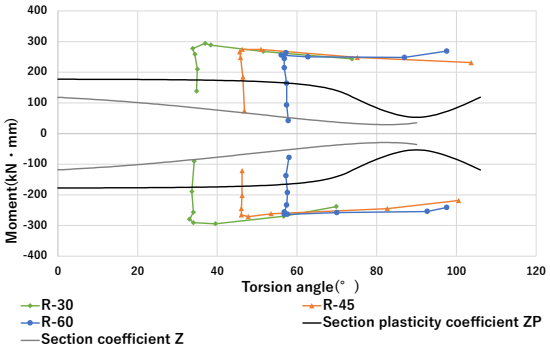

Fig. 20(b). Envelope curve of Moment-Torsional angle

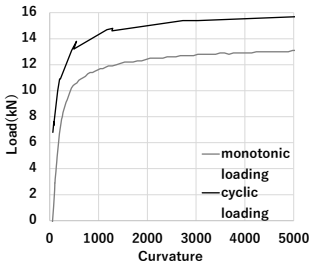

Fig. 21(a). Load-Curvature curve of R-30

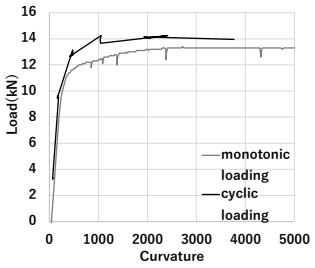

Fig. 21(b). Load-Curvature curve of R-45

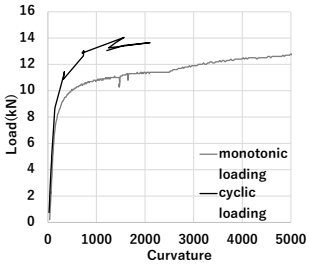

Fig. 21(c). Load-Curvature curve of R-60

Table 5. Hardening rate of TSDs.

Initial torsional angle (°)	Stable load of monotonic experiment (KN)	Stable load of cyclic experiment (KN)	Hardening (%)
30	12.8	15.1	15.0
45	12.6	14.0	10.1
60	10.8	13.3	19.1

5 Conclusion and future reservation

As a damage detection system, the frame experiment with a square rod is carried out and its tracking characteristic with drift angle is proved. After that, it is necessary to carry out dynamic load tests on the damage detection system， which installs the electronic components such as the thermoelectric device and Raspberry Pie on the square rod. This will be used to prove the effectiveness of the detection and communication functions of the damage detection system.

Through the TSDs experiment, the mechanical properties of large-angle torsion members are preliminarily discussed. The load is related to the torsional angle of the section and the hardening effect of the material is reduced due to the torsional angle of the section. After that, it is necessary to add the dynamic load test of TSDs to verify the TSD's plastic thermal behavior.

6 References

1. Japan Building Disaster Prevention Association (1998) Hisaikenchiku Oukyukikendohantei Manyuaru, Tokyo, Japan.
2. Japan Building Disaster Prevention Association (2016) Shinsaikenchikubutsuno hisaidokubunhanteikijun Oyobifukkyuuhijutsushishin, Tokyo, Japan.
3. Sakiyama N, Iwasaki E, Mori K and Ito T (2022) Damage Evaluation Method Based on Heat Generation Characteristics of Steel under Cyclic Bending Stress, Journal of Structural and Construction Engineering (Transactions of AIJ), Vol.87, No.796, pp.534-543
4. 4. Riku Fujie, Natsuhiko Sakiyama, Seine Kono, Kenjiro Mori, and Takumi Ito: DAMAGE EVALUATION METHOD OF STEEL DAMPERS SUBJECTED TO SEISMIC RESPONSE BEHAVIOR BY USING MICROCOMPUTER， ASEA-SEC-6 RAD-02-1~6， 2021.8
5. Ito T, Kono S, Fujie R (2022) Feasibility Study on Damage Monitoring System Using Thermo-Electric Conversion Method for Damaged Ductile Frames with Knee Brace Damper Installed, Summaries of Technical Papers of Annual Meeting (Transactions of AIJ)
6. Toyosada M, Gotoh K and Sagara K (1991) Temperature Rise Distribution near a Crack Tip due to Plastic Work under High Loading Rate. Journal of the Society of Naval Architects of Japan,651-663
7. Nakashima M, Sugaya M, Satoh Y, Suita K, Hokoi, S and Harada K (2002) Correlation Between Plastification and Temperature of Steel Moment Connection.Part1. Temperature Rise of Steel Beam due to Heat Generated by Plastification, Proceedings of the Architectural Research Meeting, Kinki Chapter, Architectural Institute of Jpan,173-176
8. Architectural Institute of Japan (2017) AIJ recommendations for the plastic design of steel structures, Tokyo, Japan.